Quasi-continuous burst-mode laser for high-speed planar imaging

Mikhail N. Slipchenko,[1] Joseph D. Miller,[2] Sukesh Roy,[1] James R. Gord,[3] Stephen A. Danczyk,[4] and Terrence R. Meyer[2,*]

[1]*Spectral Energies, LLC, Dayton, Ohio 45431, USA*

[2]*Department of Mechanical Engineering, Iowa State University, Ames, Iowa 50011, USA*

[3]*Air Force Research Laboratory, Propulsion Directorate, Wright-Patterson AFB, Ohio 45433, USA*

[4]*Air Force Research Laboratory, Propulsion Directorate, Edwards AFB, California 93524, USA*

**Corresponding author: trm@iastate.edu*

Received January 25, 2012; revised February 9, 2012; accepted February 10, 2012; posted February 10, 2012 (Doc. ID 162086); published April 10, 2012

The pulse-burst duration of a compact burst-mode Nd:YAG laser is extended by one order of magnitude compared to previous flashlamp-pumped designs by incorporating a fiber oscillator and diode-pumped solid-state amplifiers. The laser has a linewidth of <2 GHz at 1064.3 nm with 150 mJ per individual pulse at 10 kHz. The performance of the system is evaluated by using the third-harmonic output at 354.8 nm for high-speed planar laser-induced fluorescence of formaldehyde in a lifted methane-air diffusion flame. A total of 100 and 200 sequential images of unsteady fluid-flame interactions are acquired at repetition rates of 10 kHz and 20 kHz, respectively.

OCIS codes: 120.1740, 140.3538, 300.2530.

Understanding gas-phase combustion reactions in turbulent flows requires high-speed planar imaging with multi-kHz frame rates. Metal-vapor [1] or diode-pumped solid-state (DPSS) [2,3] lasers, can produce kHz-rate pulse sequences lasting several seconds or longer with energies limited to ~10 mJ per individual pulse. After frequency conversion to the ultraviolet for accessing electronic molecular transitions, this laser energy is reduced even further and limits the range of gas-phase chemical species that can be investigated. The introduction of burst-mode laser technology, which included the use of repetitively Q-switched Ruby lasers [4], Nd:YAG clusters [5], and pulse-burst laser amplifiers [6], significantly advanced high-speed planar laser-induced fluorescence (PLIF) imaging of gas-phase, chemically reacting flows. These laser sources can reach energies of 100's of mJ per individual pulse, but they have been limited to only a few pulses in the case of repetitively Q-switched Ruby lasers [4] or Nd:YAG clusters [5], or they have been limited to a burst duration of 1-2 ms in the case of pulse-burst laser amplifiers [7]. The time dynamics of many reacting flows of practical interest, however, can have characteristic oscillation periods of 3 ms or more [8], and it is important to extend the burst duration by at least an order of magnitude to enable studies of turbulent time dynamics for a wide range of chemically reacting flows.

In the current work we exceed the burst duration achieved by previous flashlamp-based pulse-burst lasers by (i) utilizing a fiber laser as the master oscillator, which reduces the initial gain required in the amplifier chain and provides short pulses with high spatial mode quality and low divergence; (ii) incorporating an electro-optic modulator (EOM) that reduces amplified spontaneous emission (ASE) and is more flexible and robust compared to previously used phase-conjugate mirrors based on stimulated Brillouin scattering [9]; and (iii) employing high gain at long burst durations with diode-pumped Nd:YAG amplifiers, which have an order of magnitude higher efficiency compared to flashlamp-pumped amplifiers and are not limited by the explosion energy of the flashlamps. Hence, the advantages of continuously pulsed fiber-laser and DPSS technologies are combined with burst-mode strategies to achieve an order of magnitude increase in burst duration with only a few amplification stages and reduced electrical energy consumption, resulting in a small system footprint. The capability of this new quasi-continuous burst-mode laser (QCBML) is demonstrated by high-speed (10–20 kHz) PLIF imaging of formaldehyde (CH_2O), an important intermediate species in combusting flows [10], with burst durations of 10 ms. Because of the characteristics of diode-pumped amplifier stages, as discussed below, even longer burst durations of tens of milliseconds are possible with additional amplifier stages. Although not demonstrated here, the laser energies achievable with this new laser architecture can also be used for Rayleigh scattering [11], as well as for pumping an optical parametric oscillator (OPO) to access a variety of other combustion intermediates, such as CH [12], OH [13], and NO [14].

A schematic diagram of the QCBML system for PLIF imaging is shown in Fig. 1. A commercial pulsed Yb-doped fiber laser generates a continuous 100 kHz train of pulses at 1064.3 nm wavelength with per-pulse energy of 10 μJ. The fiber-laser pulse duration is 13 ns and the line width is less than 2 GHz, allowing optimal overlap with gas-phase molecular transitions at high temperature. The utilization of a polarization-maintaining single-mode fiber results in a Gaussian beam profile with an M^2 factor of 1.3. To control the pulse-train repetition rate, the output of the fiber is collimated and directed into a pulse picker based on a 1 MHz bandwidth EOM. The EOM is used in a double-pass configuration along with an optical isolator (see Fig. 1), resulting in an extinction ratio of 2×10^3. The high extinction ratio serves to completely suppress ASE from the fiber laser so that the pulse train can be effectively amplified to a high level within the amplifier chain. The burst from the fiber amplifier is then passed through a spatial filter before being

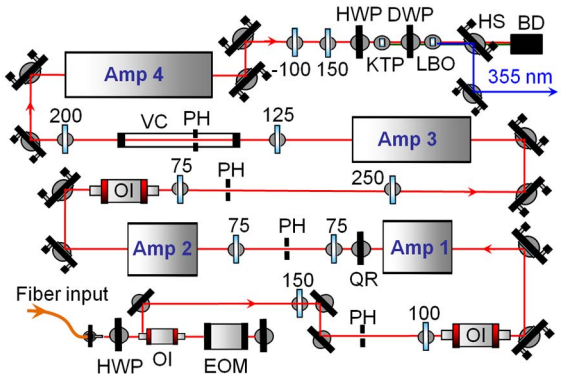

Fig. 1. (Color online) Optical layout of quasi-continuous burst-mode laser system. Symbols: OI-optical isolator, EOM-electro-optic modulator, PH-pinhole, HWP-half-wave plate, DWP-dual-wavelength wave plate, QR-quartz rotator, VC-vacuum cell, HS-harmonic separator, and BD-beam dump. Numbers are focal lengths of spherical lenses.

amplified in two small 2 mm diameter Nd:YAG-rod diode-pumped amplifiers. To prevent build-up of ASE, a relay optical arrangement with a spatial filter is placed between the amplifiers. To compensate for thermally induced birefringence, a quartz rotator is placed between the two amplifiers. The pulse train is amplified by an additional 5 mm diode-pumped amplifier that is separated from the initial two stages by an optical isolator and a spatial filter to avoid feedback and reduce build-up of ASE. To boost the final energy of the pulse burst, a low-gain, high-power, 9.5 mm flashlamp amplifier stage is used. For extended burst durations, this low-gain stage is a cost effective means of achieving two-fold energy gain with a reasonable electrical and thermal loading. Because of the high pulse energy entering this final amplification stage, a spatial filter is installed inside a custom vacuum cell to prevent air ionization in the beam focus. The amplifiers are fired at 0.5 Hz repetition rate to allow thermal relaxation of the Nd:YAG rods. Finally the fundamental output is converted via third-harmonic generation (THG) to 354.8 nm by using KTP type II and LBO type I crystals for doubling and tripling, respectively. To control the fundamental beam polarization for optimal THG generation, a dual-wavelength wave plate is used between the two nonlinear crystals. The entire optical layout occupies a 3×2 ft^2 area.

Figure 2 shows spontaneous emission (SE) time profiles from the diode- and flashlamp-pumped amplifiers. SE is proportional to the amount of stored energy inside the Nd:YAG rods and, therefore, can be used to approximate the amplification gain profile. Figure 2(a) shows that diode bars can produce up to 50 ms flat gain profile at low current; however, because of a temperature-induced shift in the diode-bar output wavelength, the high gain is restricted to the first 10 to 20 ms. In the case of flashlamps [see Fig. 2(b)], the length of the burst is limited by the power supply used, and at high pulse energy the gain profile drops with time because of limited energy storage in the capacitor banks. Because of these limitations, the burst length in the current work was restricted to 10 ms. The limitation of burst length in the case of diode bars can be overcome by working at lower current and adding additional amplifiers or by carefully

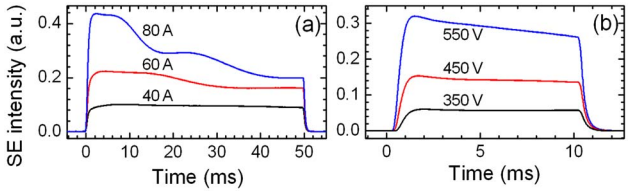

Fig. 2. (Color online) Spontaneous emission (SE) for amplifier chain as a function of time. (a) Diode-pumped amplifiers. (b) Flashlamp-pumped amplifiers.

choosing the output wavelength of the diode bars to flatten the gain profile. In the case of flashlamps, the electrical pump pulse can be extended by using a different power supply, and the energy can be maintained by adding extra capacitor banks; however, as the total electrical pump energy approaches the explosion energy of the flashlamps, a significant reduction in flashlamp lifetime may ultimately limit this strategy [15].

Figure 3 shows the gain of the amplifiers with respect to the electrical pump energy. Note that the single-pulse energy prior to the amplifier chain is 4 μJ and the burst duration is 10 ms. From Fig. 3(a) it is seen that the first two amplifiers are initially in the small-signal gain regime and begin to saturate at high pump current. The third amplifier is in the intermediate regime and the flashlamp amplifier (Amp4 in Fig. 1) is completely saturated, which is indicated by linear dependence of gain on pump energy (see Fig. 3(b)) [15]. Figure 3(c) shows the laser output energy after amplification by factors of 1225 (Amp1+Amp2), 19 (Amp3), and 2 (Amp4). Up to 150 mJ per pulse (average) is achieved in the fundamental beam at 1064.3 nm. The beam is frequency doubled with an efficiency of 56%, but the THG step is only ~20% efficient. We attribute this low efficiency to non-optimal polarization of the fundamental beam before the Type I crystal due to the Type II nature of the KTP crystal. The output pulse-to-pulse energy deviation is below 10% (standard deviation) for all three output wavelengths.

The suitability of the QCBML system for high-speed planar imaging was demonstrated in a lifted CH_4-air diffusion flame using PLIF of formaldehyde (CH_2O). The flame was stabilized over a 2 mm orifice with a flow rate of 3.06 ± 0.05 standard liters per minute, corresponding to an outlet velocity of 17 m/s and a jet Reynolds number

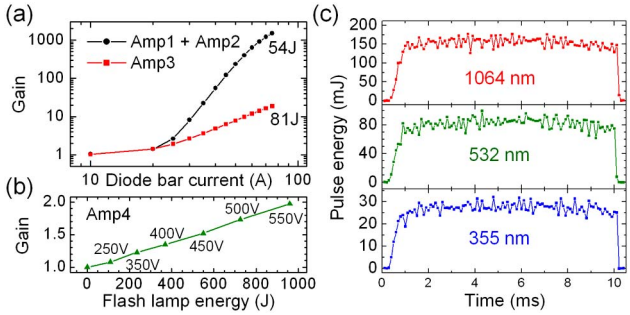

Fig. 3. (Color online) Amplifier-chain performance. (a) Diode-pumped amplifier gain as a function of pumping current. (b) Flashlamp-pumped amplifier gain as a function of flashlamp pump energy. (c) Energy distribution in the burst at 10 kHz at fundamental, second-, and third-harmonic wavelengths. The pulse-to-pulse energy deviation is below 10%.

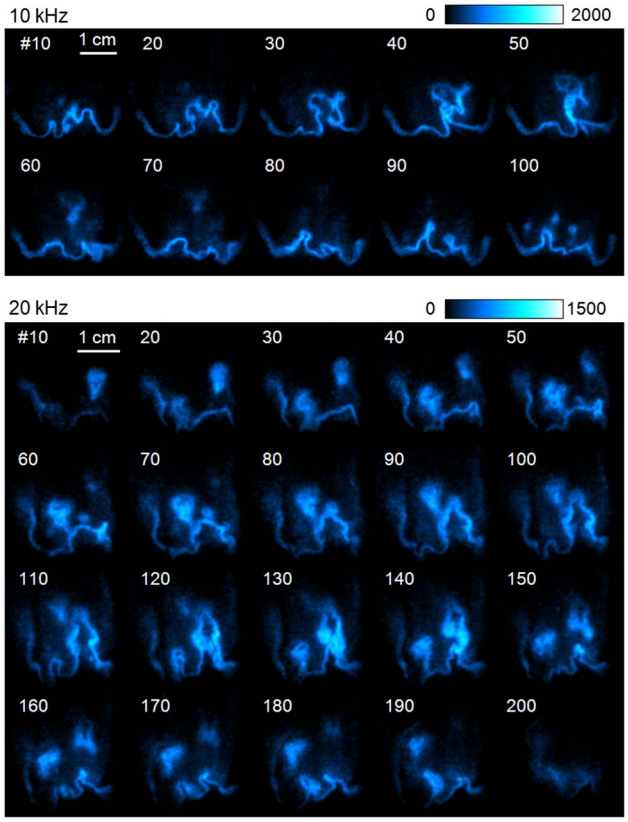

Fig. 4. (Color online) 10 ms duration PLIF imaging of CH_2O in a lifted CH_4-air diffusion flame at 10 kHz (upper panel) and 20 kHz (lower panel) showing every 10th image. False-color scales indicate non-normalized, background-subtracted camera counts. The full sequences for 10 kHz and 20 kHz are available online as Media 1 and Media 2, respectively.

of ~2000. The flame is lifted from the jet exit and exhibits a turbulent stabilization region which has been the subject of numerous investigations at low repetition rate [16].

The excitation scheme at 354.8 nm utilized ~30 mJ/pulse at 10 kHz and ~20 mJ/pulse at 20 kHz. The fluorescence signal was imaged using a Photron SA-5 high-speed camera coupled to a LaVision dual-stage high-speed intensifier. A visible Nikon Noct-Nikkor 55 mm $f/1.2$ lens was used to collect the flame image with a magnification of $1:4$ and 82.6 μm per pixel. A band pass filter from 370–450 nm was used to remove Rayleigh and Mie scatter [10]. The intensifier was operated at 67% of maximum gain with a 100 ns gate centered on the laser pulse. Two image sets collected at 10 kHz and 20 kHz are displayed in Fig. 4, showing only 10 and 20 of the 100 and 200 sequential images, respectively, with full sequences available online as media files. The laser sheet is positioned near the periphery of the jet to capture transient instabilities in the flame layer. The extended record length allows imaging of the complete detachment and reattachment of the flame layer in the stabilization region for both sets of images. By comparison, other burst-mode PLIF systems have demonstrated only 1 ms of record length [7, 17], equal to the time separating any two images in the 10 kHz sequence presented in Fig. 4. The typical signal-to-noise ratios (SNRs) for the current PLIF signals relative to spatial noise in the background are 47:1 at 10 kHz and 40:1 at 20 kHz without pixel binning. This is similar to the SNR reported elsewhere for 1 ms duration, 10 kHz burst-mode CH_2O-PLIF images collected with 5×5 pixel binning and a similar field of view [17].

In conclusion, the use of fiber and diode-pumped solid-state technology has allowed the duration of burst-mode laser imaging to be extended by an order of magnitude to 10 ms, with hundreds of pulses per burst and with per-pulse energy up to 150 mJ at 1064.3 nm. This system fills the gap between low kHz-rate, continuously pulsed systems and MHz-rate, short pulse train duration burst-mode laser systems and can monitor both low-frequency instabilities and high-speed reacting fluid dynamics. Because the number of amplifiers in this approach is scalable, additional low-gain diode-bar or flashlamp-pumped amplifiers can potentially be added to increase useful repetition rates to 100's of kHz and to extend burst durations up to tens of milliseconds.

This work was funded by the Air Force Research Laboratory (AFRL) under contract No. FA8650-10-C-2008 and by the Air Force Office of Scientific Research (Dr. Chiping Li, Program Manager). The authors are grateful for the technical assistance of C. Dedic of Iowa State University, as well as for valuable discussions with N. Jiang of Spectral Energies, W. Lempert of The Ohio State University, and I. Leyva, D. Talley, B. Kiel, M. Lightfoot, and S.A. Schumaker of AFRL.

References

1. G. A. Ruff, L. P. Bernal, and G. M. Faeth, Appl. Opt. **29**, 4544 (1990).
2. J. D. Smith and V. Sick, Appl. Phys. B **81**, 579 (2005).
3. I. Boxx, M. Stöhr, C. Carter, and W. Meier, Appl. Phys. B **95**, 23 (2009).
4. J. M. Grace, P. E. Nebolsine, C. L. Goldey, G. Chahal, J. Norby, and J.-M. Heritier, Opt. Eng. **37**, 2205 (1998).
5. C. F. Kaminski, J. Hult, and M. Aldén, Appl. Phys. B **68**, 757 (1999).
6. P. P. Wu and R. B. Miles, Opt. Lett. **25**, 1639 (2000).
7. J. D. Miller, M. Slipchenko, T. R. Meyer, N. Jiang, W. R. Lempert, and J. R. Gord, Opt. Lett. **34**, 1309 (2009).
8. P. Weigand, W. Meier, X. R. Duan, R. Giezendanner-Thoben, and U. Meier, Flow Turbul. Combust. **75**, 275 (2005).
9. N. Jiang, M. C. Webster, and W. R. Lempert, Appl. Opt. **48**, B23 (2009).
10. C. Brackmann, J. Nygren, X. Bai, Z. Li, H. Bladh, B. Axelsson, I. Denbratt, L. Koopmans, P.-E. Bengtsson, and M. Aldén, Spectrochim. Acta **59**, 3347 (2003).
11. R. A. Patton, K. N. Gabet, N. Jiang, W. R. Lempert, and J. A. Sutton, Appl. Phys. B **106**, 457 (2011).
12. J. D. Miller, S. R. Engel, T. R. Meyer, T. Seeger, and A. Leipertz, Opt. Lett. **36**, 3927 (2011).
13. J. Sjöholm, E. Kristensson, M. Richter, M. Aldén, G. Göritz, and K. Knebel, Meas. Sci. Technol. **20**, 025306 (2009).
14. N. Jiang and W. R. Lempert, Opt. Lett. **33**, 2236 (2008).
15. W. Koechner, *Solid-State Laser Engineering*, 6th ed. (Springer Science+Business Media, Inc., New York, 2006).
16. K. A. Watson, K. M. Lyons, C. D. Carter, and J. M. Donbar, Proc. Comb. Inst. **29**, 1905 (2002).
17. K. N. Gabet, R. A. Patton, N. Jiang, W. R. Lempert, and J. A. Sutton, Appl. Phys. B (2012).